A Complete and Non-Overlapping Tracing Algorithm for Closed Loops

Wu, Shin-Ting [1]

UNICAMP - State University of Campinas
Electrial and Computer Engineering Faculty
Dept. Computer Engineering and Industrial Automation
P.O.Box 6101
13083-970 - Campinas, SP, Brazil
{ting}*@dca.fee.unicamp.br*

Osmar Aléssio

UNINCOR - University Valley of Green River
Institute of Mathematics
{osmaralessio}*@yahoo.com.br*

Sueli I. R. Costa

UNICAMP - State University of Campinas
Institute of Mathematics
sueli*@ime.unicamp.br*

Abstract

A procedure for tracing completely closed loops given implicitly by the intersection of two regular surfaces, without resorting to the parametric domain subdivisions or resulting in arc overlapping, is presented. Our primary hypothesis is that the rotation index, a global geometrical property, may be a useful complementary tool to the local differential geometrical properties for improving the efficiency of the well-known marching-based surface–surface intersection algorithms. To validate this hypothesis, we devised a novel approach for incrementally computing the rotation index of a closed plane curve given implicitly while the curve is traced. Moreover, we also proposed its integration in a marching procedure that employs adaptative circular steps.

Key words: Rotation index, Regular closed plane curve, Surface–surface intersection, Marching-based algorithm, Geometric modeling.

[1] Corresponding author

1 Introduction

The main motivation of this paper is the problem of tracing, without overlapping, a closed curve given implicitly by surface–surface intersection (SSI). SSI is a fundamental problem in computational geometry and geometric modeling of complex shapes. For general parametric surface intersections, the most commonly used methods include subdivision [4,10] and marching [2,3].

Marching-based algorithms begin by finding a starting point on the intersection curve, and proceed to march along the curve. Local differential geometric properties are applied to adaptively determine the marching steps [1,4,14,17,18]. Because that the intersection of two regular surfaces may be closed loops, stopping conditions at the starting point are necessary to avoid overtracing. By a loop, we mean the intersection curve whose pre-image in the both parametric domains of the intersecting surfaces is a closed (plane) curve [12]. Traditionally, before any tracing is carried out, the loops are detected and broken into a set of open branches, for which the stopping condition consists simply in reaching either the parametric domain border or (rarely) any singular point [9,11,12,13]. In this work, we present a novel technique that applies the rotation index, namely the number of times that the tangent vectors of a plane curve turns 360 degrees, to appropriately trace it **continuously**, without resorting to domain partitioning. With this technique, we may spare the pre-processing (loop detection and domain subdivision) and the post-processing (sorting of the separately traced point sequences) that are usually required.

A *regular closed plane curve* of class $C^{(k)}$ is given by a parameterization $c\colon [a,b] \rightarrow R^2$ with continuous derivatives up to order k such that the first order derivative $\dot{c}(t) = c^{(1)}(t) \neq 0\ \forall t$, and $c(t)$ and all its derivatives up to order k agree at a and b; that is, $c(a) = c(b)$ (closeness condition), $\dot{c}(a) = \dot{c}(b)$ (tangent matching condition), ..., $c^{(k)}(a) = c^{(k)}(b)$. This set of conditions is equivalent to say that c is a periodic $C^{(k)}$ function of period $(b-a)$.

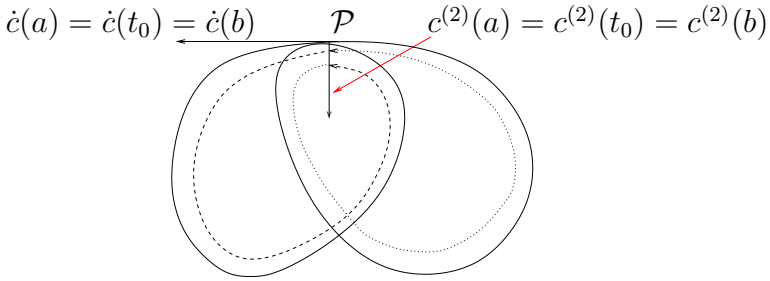

Figure 1. Overtracing the terminating point.

Figure 1 illustrates a case such that the local geometrical conditions do not suffice for getting the terminating point. Starting the tracing at $\mathcal{P} = c(a)$, the closeness and the tangent matching conditions are satisfied when $\mathcal{P} = c(t_0)$ of the curve is passed (dashed line). However, the tracing should not stop, because one loop $c|[t_0, b]$ is still

missing (dotted line). If the rotation index 2 of the curve is considered, the check of the rotation of the tangent vectors may be enough for knowing when to stop to obtain a complete and non-overlapping tracing.

Being the rotation index a global geometrical property, which is invariant under a large range of deformations, it is less sensitive to the local relative spatial placements of the traced points, as are the local geometrical properties. If the rotation index of the curve is known a priori, approaching the starting point may be easily checked with the help of the number of turns the tangent vectors rotate along the tracing curve. We also advocate that the rotation index may be useful in adjusting the tracing step sizes. Larger step size are computationally more efficient, but tends to overcross the starting point. Thus, with use of the rotation index, one may reduce the marching step size only in the vicinity of potential terminating points for appropriately stopping the tracing.

The standard definition of the rotation index involves an integration of the curvature (and hence, the second order derivatives) which requires the explicit parameterization of the curve. No methods are known in the literature that can estimate the rotation index of a curve given implicitly by the intersection of two surfaces. The primary contribution of this paper is to present an expression that relates the rotation index of a regular closed plane curve with its m positively, n negatively oriented parameterized loops and k_j branch points with (net) multiplicity greater than two

$$n_c = (m - n) - \sum_{j=1}^{l} k_j. \tag{1}$$

The concepts of parameterized loops and net multiplicity are explained in Section 2. Essentially, they are defined on the basis of the branch (transversal self-intersection) points. The complete proof of the relation is given in Section 3. This relation (Eq. 1) provides an alternative way to compute the rotation index of a closed curve without knowing its parametric representation. It tells us that, from a set of non-overlapping oriented parameterized loops that builds a regular closed plane curve, one can determine its rotation index. On the basis of this equation, we devise an algorithm that can compute the rotation index of a closed curve given implicitly by the intersection of two regular surfaces, if the curve is **continuously** traced starting at a point that does not lie in the vicinity of a self-intersection point. The branch points can be reliably computed, since they must be the pre-images of the intersection points where the surfaces are tangent.

The second contribution of our work is the integration of the novel rotation index algorithm in a marching-based algorithm for ensuring complete continuous tracing. We used the circular-step-marching procedure proposed by Wu and Andrade [18], since it works well when the curve contains singularities up to fourth order contact without abrupt change of normal directions. The key point for the integration con-

sists in incrementing or decrementing the rotation index whenever a pair of branch points is matched under the restriction that its associated parametric loop does not overlap any previously detected parameterized loops. Section 4 gives an algorithm that uses the estimated rotation indices to select the potential vicinities of the starting point. Only in the potential vicinities, the step size is diminished for carefully monitoring the local geometrical properties. It is worth remarking that only in one of these potential vicinities there is a point that satisfies the local geometric conditions. Hence, for the sake of performance, the step size is restored whenever the tracing leaves an incorrect vicinity.

Some numerical results are given in Section 5 and our concluding remarks are made in Section 6.

2 Rotation Index and Self-intersection Points

The *rotation index* or *turning number* of a regular closed plane curve c: $[a, b] \rightarrow R^2$ is the algebraic number n_c of times the (oriented) tangent vector $\dot{c}(t)$ of a curve rotates along the curve with respect to a fixed axis [5,7,15]. The rotation indices of the curves in Figure 2.a, Figure 2.b, Figure 2.c are, respectively, 2, -1, and 0.

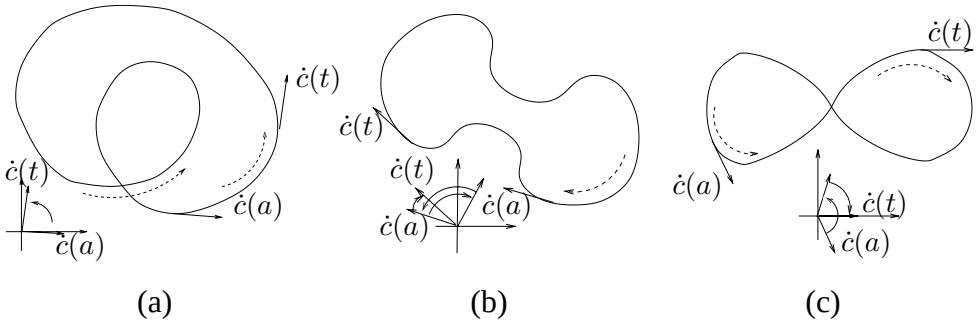

Figure 2. Rotation index.

Let $c(t)$ be a regular closed plane curve parameterized by a generic parameter t, it is possible to obtain a curve $c(s)$ parameterized by arc length s which has the same trace as $c(t)$. The curvature $k(s)$ can be defined as the derivative $\frac{d\theta(s)}{ds}$, where θ is the angle that the tangent vector makes with the x axis. Since $\frac{ds}{dt} = |\dot{c}(t)|$, we may write

$$\int_0^w \kappa(s)ds = \int_a^b \kappa(t)|\dot{c}(t)|dt = \theta(a) - \theta(b) = n_c 2\pi,$$

from which we derive an expression for the rotation index of c by the integer

$$n_c = \frac{1}{2\pi} \int_a^b \kappa(t)|\dot{c}(t)|dt. \tag{2}$$

As we see next, this integer number is invariant under the regularly homotopic deformations and we use this fact to derive Eq. 1.

Definition 1 *[8] Two regular curves $c_1(t)$ and $c_2(t)$ are said to be* regularly homotopic, *if there exists a continuous function $\mathcal{H}$ such that each $\mathcal{C}_u(t) = \mathcal{H}(t, u)$, $u \in [0, 1]$, is a regular curve and $\mathcal{C}_0(t) = c_1(t)$ and $\mathcal{C}_1(t) = c_2(t)$ are the given initial curves. $\mathcal{H}$ is a continuous deformation from $c_1(t)$ to $c_2(t)$ and is called a* regular homotopy.

Proposition 2 *[5] Two regular closed plane curves are regularly homotopic, if and only if, they have the same rotation index.*

A consequence of this proposition is that there are only three classes of curves to one of which any regular closed plane curve is regulaly homotopic.

Proposition 3 *[5] Every regular closed plane curve is homotopic to one of the following curves:*

(1) a simple curve positively or negatively oriented (Figure 3a),
(2) the eight-shaped curve (Figure 3b), and
(3) a C_n curve with n loops all positively or negatively oriented (Figure 3c).

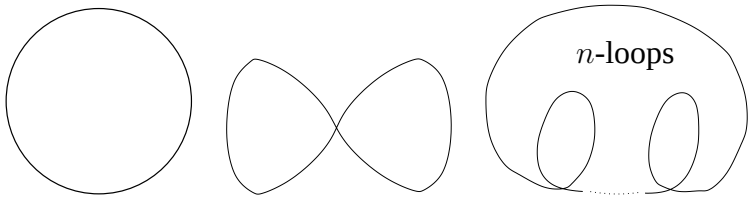

Figure 3. Three classes of closed plane curves.

Hence, if we know how to reduce a closed curve to one of the three patterns of curves, the computation of the rotation number is trivial. However, for deriving the rotation index from the number of the singular points of a curve, we must consider the rotation index of piecewise regular plane curves.

Definition 4 *[8] Let $c\colon [0, w] \to R^2$ be a continuos function, with continuous derivatives up to order k and $c\prime(t) \neq 0$, except at a finite number of points, $a_0 = 0 < a_1 < a_2 < \cdots < a_k = w$, such that there exist the right and left hand*

limits ($\dot{c}(a_i{}^+) = \lim_{t\to a_i{}^+} \dot{c}(t)$ *and* $\dot{c}(a_i{}^-) = \lim_{t\to a_i{}^-} \dot{c}(t)$*) for the tangent vector at* a_i*. Then we say that* c *is a* piecewise regular plane curve. *When* $c(0) = c(w)$*, it is also a closed curve.*

For a piecewise regular closed plane curve, the rotation index is defined by adding the "jump" angles at the singularities as follows.

Definition 5 *[8] Let* $c\colon [0, w] \to R^2$ *be a piecewise regular closed plane curve. Let* $a_0 = 0 < a_1 < a_2 < \cdots < a_k = w$ *be a partition such that* $c|[a_i, a_{i+1}]$ *is regular and* α_i*,* $-\pi < \alpha_i \leq \pi$*, denotes the* oriented exterior angle *from* $\dot{c}(a_i^-)$ *to* $\dot{c}(a_i^+)$*,* $1 \leq i \leq k-1$*, and* α_k *the angle from* $\dot{c}(a_k{}^-)$ *to* $\dot{c}(a_k{}^+) = \dot{c}(a_1{}^+)$*. The number*

$$n_c = \frac{1}{2\pi} \sum_{i=1}^{k} \int_{a_i}^{b_i} \kappa(t)|\dot{c}(t)|dt + \frac{1}{2\pi} \sum_{i=1}^{k} \alpha_i. \tag{3}$$

is the rotation index *of* c*.*

The magnitude of the oriented exterior angle $|\alpha_i|$, in radians, can be determined by

$$cos\alpha_i = \frac{\dot{c}(a_i^-) \cdot \dot{c}(a_i{}^+)}{|\dot{c}(a_i^-)||\dot{c}(a_i^+)|}. \tag{4}$$

and its sign, by the sign of the third coordinate of the cross product $\dot{c}(a_i{}^-) \times \dot{c}(a_i{}^+)$.

The next proposition establishes that n_c is always an integer, as it is for regular closed plane curves. The proposition also tells us that $|n_c|$ is invariant under isometries of R^n and change of variables wich preserve orientatiton.

Proposition 6 *[8] The rotation index* n_c *of a piecewise regular closed plane curve is an integer. Moreover,* n_c *is invariant under orientation-preserving change of variables or direct isometries of* R^n*. An orientation-reversing change of variables or reflections in* R^n *will change the sign of* n_c*.*

For our algorithm we also use the fact stated in the next proposition.

Proposition 7 *[7] The rotation index of a piecewise regular simple closed plane curve is* $\pm$ *1, where the sign depends on the orientation of the curve.*

We introduce the following definition to characterize and classify the self-intersection points.

Definition 8 *Let* $c\colon [a, b] \to R^2$ *be a regular closed curve. A point* $\mathcal{P} = c(t) = (x(t), y(t))$ *is a* self-intersection point*, if there are at least two parameters* $t_1, t_2 \in [a, b]$*,* $t_1 \neq t_2$*, such that* $\mathcal{P} = c(t_1) = c(t_2)$*. The* multiplicity *of* $\mathcal{P}$ *is the number*

of points in $c^{-1}(P)$*. A point is said to be* simple *(*multiple, double, triple*) if its multiplicity is 1 (>1, 2, 3).*

We further distinguish the self-intersection points at which the curve **effectively crosses** itself either transversally or even with equal unit tangents.

Definition 9 *Let* $c\colon [a,b] \to R^2$ *be a regular closed plane curve and let* $\mathcal{P} = c(t_1) = c(t_2)$ *be a self-intersection point. If the orientation from the vector* $\dot{c}(t_1 - \varepsilon)$ *to the vector* $\dot{c}(t_2 - \psi)$ *and the orientation from the vector* $\dot{c}(t_1 + \varepsilon)$ *to the vector* $\dot{c}(t_2 + \psi)$ *are the same for small and positive* ε *and* ψ*, then we say that* $\mathcal{P}$ *is a* branch point relatively to $\{t_2,t_1\}$ *and we call* $\{t_2,t_1\}$ *a* branch pair. *Otherwise,* $\mathcal{P}$ *is denominated a* tangential point relatively to the tangential pair $\{t_2,t_1\}$.

Algebraically, the condition for being a branch point may be translated as

$$[\dot{c}(t_1 - \varepsilon) \times \dot{c}(t_2 - \psi)] \cdot [\dot{c}(t_1 + \varepsilon) \times \dot{c}(t_2 + \psi)] > 0. \tag{5}$$

Observe that a transversal double point (a point at which the tangents are not coincident) is a branch point (Figure 4a). But, if we have just one tangent at a double point, we may have either a branch (Figure 4b) or a tangential point (Figure 4c).

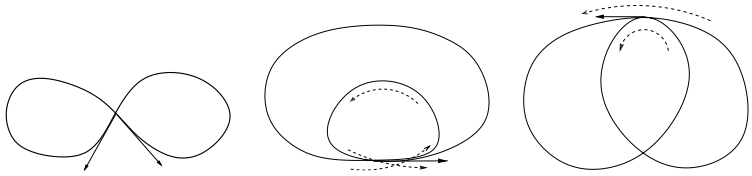

(a) (b) (c)

Figure 4. (a) A transversal branch point; (b) A branch point with coincident tangents; (c) A tangential point.

As we will see in Proposition 12 the tangential points can be disregarded in the computation of the rotation index. Through a regular homotopy, we may slightly move a small arc containing a tangential point away from the remaining part of the curve (Figures 5 and 8). In this process, we reduce the multiplicity of a self-intersection point, without affecting the rotation index of the curve. This motivates us to introduce the definitions of *net multiplicity* and *parametrized loop.*

Definition 10 *Let* $\mathcal{P}$ *a multiple point and* $c^{-1}(\mathcal{P}) = \{ t_1, \cdots, t_j, \cdots, t_k\}$*.* t_j *is called a* branch generator *if there exists* $t_l \neq t_j$ *such that* $\mathcal{P}$ *is a branch point relatively to* $\{t_j,t_l\}$*. The* net multiplicity *of a point* $\mathcal{P}$ *on the curve is the number of points in* $c^{-1}(P)$ *which are branch generators.*

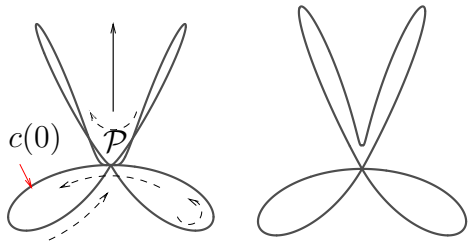

(a) (b)

Figure 5. A point with multiplicity 4, but net multiplicity 3.

Figure 5.a exemplifies a curve $c\colon [0,1] \to R^2$ with two double points (multiplicity 2) and a point $\mathcal{P}$ with multiplicity 4, since $c^{-1}(\mathcal{P}) = \{t_1, t_2, t_3, t_4\}$. We may, however, apply a regular homotopy to a vicinity of $c(t_2)$ to "pull" it slightly in the direction of the solid arrow and remove a tangential pair (Figure 5.b). The net multiplicity of $\mathcal{P}$ is, therefore, 3. Note that the rotation index of both curves is 2.

Definition 11 *Let $\mathcal{A} = [t_0, t_1) \cup [t_2, t_3) \cup \cdots \cup [t_{n-1}, t_n)$, $a < t_0 < t_1 < t_2 < t_3 < \cdots < t_{n-1} < t_n < b$, where t_1, t_2, $\cdots$ t_{n-1}, t_n are the branch generators of c. The restriction $c\colon \mathcal{A} \to R^3$ is called a* parametrized loop *if the following conditions are fulfilled:*

(1) $c|\mathcal{A}$ *has net multiplicity equal to 1, for all* t*,*
(2) $c(t_1) = c(t_2)$, $c(t_3) = c(t_4)$, $c(t_5) = c(t_6)$, $\cdots$, $c(t_{n-2}) = c(t_{n-1})$,
(3) $c(t_0) = c(t_n)$,
(4) t_0 *and* t_n *is a branch pair.*

If there is no branch generator in c, the above conditions will not be violated and we will assume that c is itself a parametrized loop.

If $c(t)$ is a regular closed plane curve, each parametrized loop $\mathcal{L}$ is a piecewise regular closed plane curve, which has no self-intersections except at the tangential points. The rotation index (defined by Eq. 3) of $\mathcal{L}$ is either 1 or -1 according this loop is either positively or negatively oriented.

Whenever a starting point and the orientation are fixed, we can order all the branch generators sequential and periodically along the parametric domain and use them to partition this domain into non-overlapping (with no arc intersections) sub-intervals such that each of them is delimited by branch pairs. This partition is unique and each oriented parametrized loop corresponds to a subset of these sub-intervals. Besides, the sum of the rotation indices of the oriented parametrized loops obtained from any partition must be the same. In Figure 6 we illustrate four different partitions of a curve in parametrized loops. The branch pairs are drawn in distinguishing shapes and their corresponding parametrized loops in lines with different width. Observe that, although the curve is represented by different functions

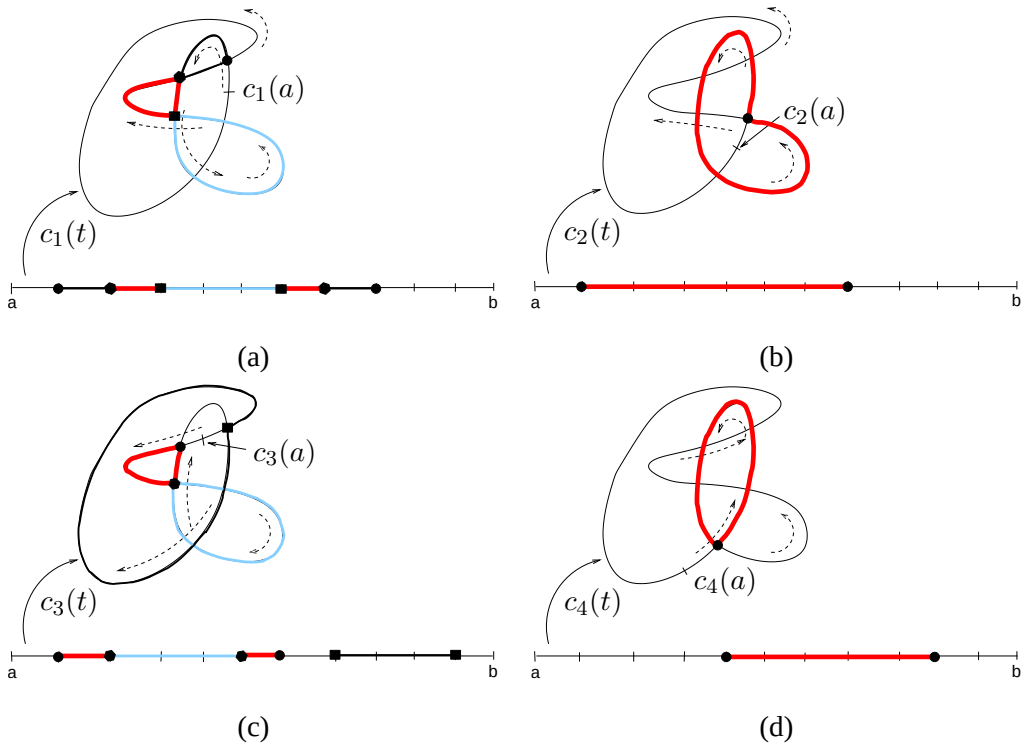

Figure 6. Different parametric partitions for the same curve.

c_i: $[a, b] \rightarrow R^2$ having different starting point $c_i(a)$, the sum of the rotation indices of the parametrized loops is 2 for all of them.

To proceed to relate the rotation index of a curve with its parametrized loops, we first point out that if a branch point has multiplicity two, the algebraic sum of oriented exterior angles at $\mathcal{P}$ relatively to the two adjacent loops is zero (since we have crossing tangents and the exterior angles have reversal orientation). This will imply that for a closed curve which has only multiple points of this type (simple crossings) the rotation index is just the algebraic sum of the indices of its parametrized loops (Proposition 13). Note that the curve given in Figure 6 is an example of this case.

If the net multiplicity of a point $\mathcal{P}_j$ is greater than 2, the algebraic sum of the oriented exterior angles of all its q adjacent parametrized loops is a (signed) integer multiple k_j of 2π. This implies that we must include in the equation given in Proposition 13 a correction factor $\sum_{j=1}^{l} k_j$, where l denotes the number of branch points with net multiplicity greater than two. A general expression (Eq. 1) that relates the rotation index and the number of oriented paremetrized loops is then reached (Proposition 14).

Let's give a geometrical view of this correction factor. For a point $\mathcal{P}$ with net multiplicity greater than 2 in $c(t)$, one can always perturb the vicinity of $\mathcal{P}$ through a small continuous deformation and reduce it to one of three curves listed in Proposition 3. Depending on the singularity at $\mathcal{P}$, additional loops with reversal orientation

may appear. The number of these loops corresponds to the number of complete turns we must jump to completely trace the curve $c(t)$ and they must be taken off from the algebraic sum of the individual rotation indices of parametrized loops.

Figure 7a illustrates a closed curve having two points with net multiplicity greater than 2 (m=6, n=1, k_1=0, and k_2=0) and its deformation into a C_5 curve (a closed curve with 5 loops). This result can be predicted from Eq. 1, once $n_c = (6-1) - (0+0) = 5$. Figure 7b shows a closed curve having two petal-shaped points (m=4, n=4, k_1=1, and k_2=-1) into an eight-shaped curve. The result is also predictable with use of Eq. 1 ($n_c = (4-4) - (1-1) = 0$). We also remark that, after the first deformation stage, both the curves only possess points with multiplicity at most two and in Figure 7b only two loops with reversal orientation appeared at the final stage of the deformation.

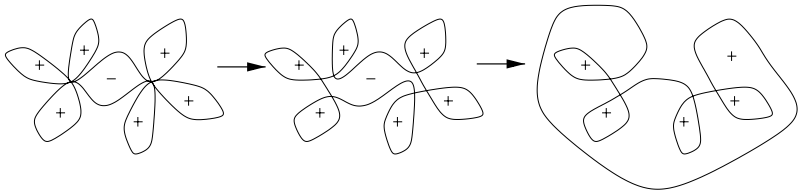

(a)

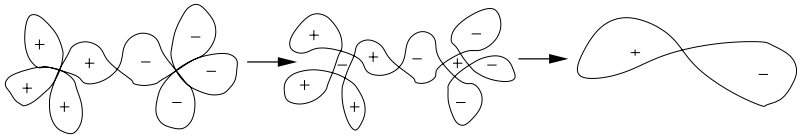

(b)

Figure 7. Regularly homotopic deformations.

3 Analysis

In this section we prove the correctness of Eq. 1. The proof, concluded in Proposition 14, is constructed from two statements to be firstly developed: Proposition 12 which ensures that the tangential pairs can be ignored in the computation of the rotation index of a closed curve and Proposition 13 which establishes the rotation index of curves with at most simple crossings.

Proposition 12 *Any regular closed curve c_1 is regularly homotopic to a curve $\mathcal{C}$ which has no tangential pairs. The new curve $\mathcal{C}$ is coincident with c_1 out of a neighborhood of the original tangential pairs.*

PROOF. Let $\mu(t)$ be a bump function that slightly displaces, without overlapping $c_1(t)$, a tangential point $c_1(t_2)$ relatively to the pair $\{t_1, t_2\}$ and its vicinity from

$c_1(t_1)$ in the direction of the curvature vector $n_1(t) = \kappa(t)n(t)$ of $c_1(t)$, such as c_2: $[a, b] \to R^2$ defined by (Figure 8)

$$c_2(t) = \begin{cases} c_1(t) & \text{if } t \in [a, t_2 - \delta], \\ c_1(t) + \mu(t)n_1(t) & \text{if } t \in (t_2 - \delta, t_2 + \delta), \\ c_1(t) & \text{, otherwise.} \end{cases}$$

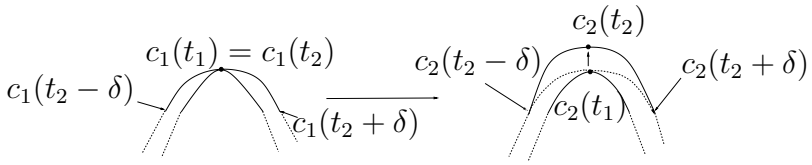

Figure 8. Slight deformation from $c_1(t)$ to $c_2(t)$.

Using the classical C^∞ Cauchy function β: $R \to R$ (Figure 9)

$$\beta(t) = \begin{cases} 0 & \text{if } t \leq 0, \\ \pm\epsilon \ \exp(-\frac{1}{t}) & \text{if } t > 0. \end{cases},$$

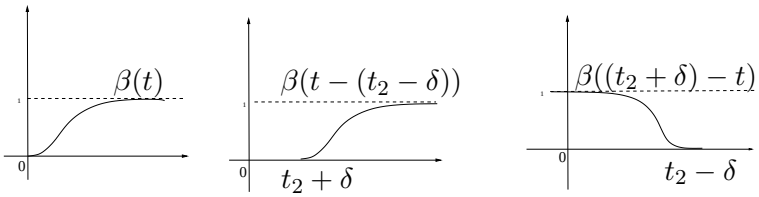

Figure 9. Cauchy function.

we define the bump function μ: $R \to R$ as follows (Figure 10)

$$\mu(t) = \beta(t - t_1).\beta(t_2 - t), \forall t \in [a, b]. \tag{6}$$

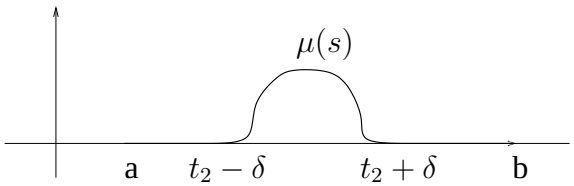

Figure 10. A bump function.

Note that $c_1(t)$ and $c_2(t)$ will not intersect in the neighborhood of t_2 by appropriately choosing the sign $\pm$ and the value of ϵ.

Hence, the function $\mathcal{H}\colon I \times I \to R^2$

$$\mathcal{H}(t,u) = \begin{cases} c_1(t) & \text{if } t \in [a, t_2 - \delta], \\ c_1(t) + u\mu(t)n_1(t) & \text{if } t \in (t_2 - \delta, t_2 + \delta), \\ c_1(t) & \text{if } t \in [t_2 + \delta, b] \end{cases}$$

with $t \in [0,1]$ can deform $c_1(t)$ into $c_2(t)$ without the tangential pair $\{t_1, t_2\}$.

$\mathcal{H}$ is a continuous function and $\mathcal{H}(t,0) = c_1(t)$, $\mathcal{H}(t,1) = c_2(t)$. Moreover, for a fixed u, $\mathcal{C}_u(t) = \mathcal{H}(t,u)$ is a regular curve. To see this, we may assume, without loss of generality, that c_1 is parametrized by its arc length. Hence, $|\dot{c}_1(t)| = 1$ and $\dot{n}_1(t) = -\kappa(t)\dot{c}_1(t)$ by the Frenet formulas. So, we have

(1) for $t \in (t_2 - \delta, t_2 + \delta)$

$$\begin{aligned} \dot{\mathcal{C}}_u(t) &= \dot{c}_1(t) + u\dot{\mu}(t)n_1(t) + u\mu(t)\dot{n}_1(t) \\ &= (1 - u\mu(t)\kappa(t))\dot{c}_1(t) + u\dot{\mu}(t)n_1(t). \end{aligned}$$

This means that for conveniently small ϵ

$$|\dot{\mathcal{C}}_u(t)|^2 = (1 - u\mu(t)\kappa(t))^2 + (u\dot{\mu}(t))^2 \geq (1 - u\mu(t)\kappa(t))^2 > 0.$$

(2) for $t \in [a, t_2 - \delta] \cup [t_2 + \delta, b]$, we can see that $\dot{\mathcal{C}}_u(t) = \dot{c}_1(t)\ \forall u$, since $\dot{\mu}(t_2 - \delta) = \dot{\mu}(t_2 + \delta) = 0$.

Once there exists a continuous function $\mathcal{H}$ such that each $\mathcal{C}_u(t) = \mathcal{H}(t,u)$, $u \in [0,1]$, is a curve from $\mathcal{C}_u(a)$ to $\mathcal{C}_u(b)$ and $\mathcal{C}_0(t) = c_1(t)$ and $\mathcal{C}_1(t) = c_2(t)$ are the given initial curves, $c_1(t)$ and $c_2(t)$ are regularly homotopic curves. From Proposition 2, we conclude that $c_1(t)$ and $c_2(t)$ have the same rotation index.

The same procedure can be applied recursively to all other tangential pairs of the original curve c_1 in order to finally get the curve $\mathcal{C}$ regularly homotopic to c_1 and without tangential pairs.

q.e.d.

Proposition 13 *Once a starting point is fixed, if all the points of a regular closed plane curve have net multiplicity at most two, then the rotation index is*

$$n_c = m - n, \tag{7}$$

where m and n are the number of positively and negatively oriented parametrized loops of this curve.

PROOF. To emphasize the geometric idea involved, let us consider first the case of a curve $c\colon [a,b] \to R^2$ with just one branch pair $\{t_1, t_2\}$, $a < t_1 < t_2 < b$. Then, according to Eq. 2

$$n_c = \frac{1}{2\pi}[\int_a^{t_1} \kappa(t)|\dot{c}(t)|dt + \int_{t_1}^{t_2} \kappa(t)|\dot{c}(t)|dt + \int_{t_2}^{b} \kappa(t)|\dot{c}(t)|dt].$$

Rearranging this sum according to its two parametrized loops $\mathcal{L}_1$ and $\mathcal{L}_2$, we have

$$n_c = \frac{1}{2\pi}[\int_{t_1}^{t_2} \kappa(t)|\dot{c}(t)|dt + (\int_a^{t_1} \kappa(t)|\dot{c}(t)|dt + \int_{t_2}^{b} \kappa(t)|\dot{c}(t)|dt)]. \quad (8)$$

Since we have crossing tangents at $\mathcal{P} = c(t_1) = c(t_2)$, for any parameterization the exterior angles of $\mathcal{L}_1$ and $\mathcal{L}_2$ at $\mathcal{P}$ have the same value α but with reversal orientation. Adding the term $\alpha - \alpha$ to the right-hand side of Eq. 8, we get

$$n_c = \frac{1}{2\pi}(\int_{t_1}^{t_2} \kappa(t)|\dot{c}(t)|dt + \alpha) + \frac{1}{2\pi}(\int_a^{t_1} \kappa(t)|\dot{c}(t)|dt + \int_{t_2}^{b} \kappa(t)|\dot{c}(t)|dt - \alpha). \quad (9)$$

According to Proposition 3, there are three classes of geometric arcs. It is then necessary to show that for all of them we may describe the rotation index of a curve as the algebraic sum of the rotation indices of its parametrized loops.

If we consider that both loops are positively oriented (Figure 11.a), then the exterior angle of one loop, say $\mathcal{L}_1$, is in the same sense (positive) and the exterior angle of another is in reversal sense (negative). It follows that the sum of terms inside each pair of parentheses in Eq. 9 corresponds exactly to the rotation index of a parametrized loop. Then, we may write n_c as a function of the rotation index of the parametrized loops $n_{c,\mathcal{L}_1}$ and $n_{c,\mathcal{L}_2}$

$$n_c = n_{c,\mathcal{L}_1} + n_{c,\mathcal{L}_2} = 2.$$

An analogous argument holds to show the proposition in the cases both loops are negatively oriented (Figure 11.b).

If we consider that both loops have reversal orientation, then the exterior angle of the positively oriented loop, say $\mathcal{L}_1$, is positive and the exterior angle of the negatively oriented loop, say $\mathcal{L}_2$, is negative. Then, the terms inside the first pair of parentheses in Eq. 9 correspond to $\mathcal{L}_1$ and inside the second pair to $\mathcal{L}_2$. Clearly,

$$n_c = n_{c,\mathcal{L}_1} - n_{c,\mathcal{L}_2} = 0.$$

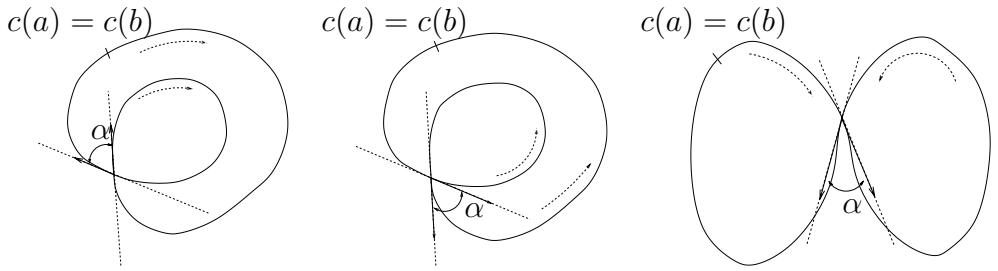

(a) (b) (c)

Figure 11. Exterior angles of parametrized loops.

This proof can be extended to a general closed curve $c\colon [a,b] \rightarrow R^2$ with at most simple crossings and $c(a) = c(b)$. Once a parameterization (also a starting point) is fixed, we consider the decomposition of c into parametrized loops $\mathcal{L}_1$, $\mathcal{L}_2$, $\cdots$, $\mathcal{L}_q$.

Let $\tilde{c} = \{t_1, \cdots, t_{k-1}\}$, $a = t_0 < t_1 < \cdots < t_k = b$, be the union of all the branch pairs of $c(t)$. The rotation index can be written as

$$n_c = \frac{1}{2\pi} \sum_{i}^{k-1} \int_{t_i}^{t_{i+1}} \kappa(t)|\dot{c}(t)|dt.$$

We may rearrange this sum taking into account the parametrized loops $\mathcal{L}_j$ of c, $j = 1, \cdots, q$, each of which is the image of $N(j)$ disjoint segments

$$n_c = \frac{1}{2\pi} \sum_{j=1}^{q} (\sum_{l=1}^{N(j)} \int_{t_{j,l}}^{t_{j,l+1}} \kappa(t)|\dot{c}(t)|dt).$$

Since each singularity of a loop consists of a simple crossing and the algebraic sum of the exterior angles of the two adjacent loops at this crossing is zero, the same reasoning of the simplest case can be applied.

Replacing conveniently each term and knowing that, by symmetry, the terms α_i are cancelled at the common image of the parametrized branch pairs, we may express the rotation index of c (with m positively oriented and n negatively oriented loops) as

$$n_c = m(+1) + n(-1) = m - n. \tag{10}$$

q.e.d.

Let us illustrate the application of Eq. 10 in the curves plotted in Figure 6. They are, in fact, the results of the partitioning of the same curve into distinct parametrized

loops. We have in (a) m=3 and n=1; (b) m=2 and n=0; (c) m=3 and n=1; and (d) m=2 and n=0, all of which lead to $n_c = 2$, as expected.

We point out in the proof of Proposition 13 one essential fact we applied in the derivation of Eq. 1: the sum of the exterior angles of two adjacent loops at a simple crossing is zero. At a point with net multiplicity greater than two, we can only assert that the sum of exterior angles of the adjacent loops is an integer multiple of 2π and this correction factor must be included in the expression of the rotation index of the curve, as we see next.

Proposition 14 *The rotation index of a regular closed plane curve c partitioned into m positively and n negatively oriented loops with l points whose net multiplicity is greater than two is given by*

$$n_c = (m - n) - \sum_{j=1}^{l} k_j,$$

where $k_j = \frac{\sum_{i=1}^{N(j)} \alpha_{j,i}}{2\pi}$ with $N(j)$ denoting the number of the parametrized loops adjacent to the branch point $\mathcal{P}_j$ and $\alpha_{j,i}$ representing the exterior angle of each of these adjacent loops.

PROOF. Let $c\colon [a, b] \to R^2$ be a regular closed plane curve with L branch points and $c(a) = c(b)$. Let $\tilde{c} = \{t_1, \cdots, t_{k-1}\}$, $a = t_0 < t_1 < \cdots < t_k = b$, be the union of all the branch pairs of $c(t)$. Then the rotation index of c can be written as

$$n_c = \frac{1}{2\pi} \sum_{r=0}^{k-1} \int_{t_r}^{t_{r+1}} \kappa(t)|\dot{c}(t)|dt.$$

We may rearrange this sum taking into account the parametrized loops $\mathcal{L}_i$ of c, $i = 1, \cdots, q$, each of which is the image of $L(i)$ disjoint intervals

$$n_c = \frac{1}{2\pi} \sum_{i=1}^{q} (\sum_{s=1}^{L(i)} \int_{t_{i,s}}^{t_{i,s+1}} \kappa(t)|\dot{c}(t)|dt). \tag{11}$$

Since each parametrized loop is a piecewise regular simple closed plane curve, its rotation index is

$$n_{\mathcal{L}_i} = \frac{1}{2\pi} (\sum_{s=1}^{L(i)} \int_{t_{i,s}}^{t_{i,s+1}} \kappa(t)|\dot{c}(t)|dt + \sum_{j=1}^{L(i)} \alpha_{j,i}) = \pm 1,$$

where $\alpha_{j,i}$ is the exterior angle of $\mathcal{L}_i$ at a singular point $\mathcal{P}_j$. From this fact,

$$\frac{1}{2\pi}(\sum_{s=1}^{L(i)} \int_{t_{i,s}}^{t_{i,s+1}} \kappa(t)|\dot{c}(t)|dt) = \pm 1 - \frac{\sum_{j=1}^{L(i)} \alpha_{j,i}}{2\pi}. \tag{12}$$

Denoting $(\pm 1)_{\mathcal{L}_i}$ the rotation index, $+1$ or -1, relative to the loop $\mathcal{L}_i$ and replacing Eq. 12 in Eq. 11, we obtain

$$n_c = \sum_{i=1}^{q}((\pm 1)_{\mathcal{L}_i} - \frac{\sum_{j=1}^{L(i)} \alpha_{j,i}}{2\pi}).$$

If c has m positively and n negatively oriented loops, we may replace the term $\sum_{i=1}^{q} (\pm 1)_{\mathcal{L}_i}$ by $m(+1) + n(-1)$ and get

$$n_c = m - n - \sum_{i=1}^{q} \frac{\sum_{j=1}^{L(i)} \alpha_{j,i}}{2\pi}.$$

Once each exterior angle $\alpha_{j,i}$ is associated to a unique branch point, we may recollect the summation in the above expression in terms of the L branch points

$$n_c = m - n - \sum_{j=1}^{L} \frac{\sum_{p=1}^{N(j)} \alpha_{j,p}}{2\pi},$$

where $N(j)$ is the number of the parametrized loops adjacent to the branch point $\mathcal{P}_j$.

The algebraic sum of the (two) exterior angles at a branch point with net multiplicity equal to two is $\frac{\sum_{p=1}^{2} \alpha_{j,p}}{2\pi} = 0$. Therefore, by considering only the l branch points with net multiplicity greater than two, we may rewrite the expression in the form (Eq. 1)

$$n_c = m - n - \sum_{j=1}^{l} k_j.$$

q.e.d.

Figure 12 shows two petal curves considered positively oriented. In Figure 12a, it is a 11-petal curve which has 8π as the sum of exterior angles of the parametrized loops at the singular point. The rotation index of the curve is, therefore, $n_c = 11 - \frac{8\pi}{2\pi} = 7$ ($m = 11$, $n = 0$ and $\sum k_j = 4$). The 6-petal curve in Figure 12b with

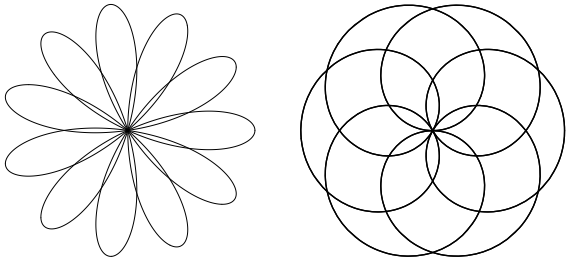

(a) (b)

Figure 12. (a) A 11-petal curve and (b) a 6-petal curve: both have rotation index 7.

the sum of exterior angles equal to -2π has also the rotation index $6 - (-\frac{2\pi}{2\pi}) = 7$ ($m = 6$, $n = 0$ and $\sum k_j = -1$).

Corollary 15 *If the algebraic sum of the exterior angles at each branch point is $\pm 2\pi$, then the rotation index of a curve may be obtained from the expression [16]*

$$n_c = (m - n) - (\mathcal{K}_1 - \mathcal{K}_2), \tag{13}$$

where $\mathcal{K}_1$ and $\mathcal{K}_2$ are the number of branch points with positive sum (2π) and the number of branch points with negative sum (-2π), respectively.

PROOF. This follows immediately from the rearrangement of the sum $\sum_{j=1}^{l} k_j$ into two groups $\mathcal{K}_1 = \sum_{j=1}^{l} k_j$ with $k_j > 0$ and $\mathcal{K}_2 = |\sum_{j=1}^{l} k_j|$ with $k_j < 0$.

q.e.d.

4 A modified Marching Algorithm

The underlying idea of Eq. 1 is that we may reduce the computation of the rotation index of a curve to the evaluation of the local behaviour of the branch points, namely we should (1) determine the number of matching branch pairs whose associated parametrized loops do not have arc intersections, and (2) distinguish the branch points that have net multiplicity greater than two for computing the total algebraic sum of exerior angles at them.

For the first item, we propose to use a stack to remember a branch generator that has been traced (push the traced branch point and its respective branch generator in the stack) and to go back to the pairing branch generator (pop all the stacked branch generators till the matched branch generator) to close a parametrized loop without overlapping the existing ones. And for the second item, we allocate a cell to each

singular point for storing its multiplicity and the algebraic sum of the exterior angles. In principle, each branch point must have at least two branch generators after completing a round along a closed loop given implicitly by two regular surfaces $\mathcal{S}_1$ and $\mathcal{S}_2$, as summarizes the following algorithm. We consider in the algorithm that the given tracing step size L in the direction of the tangent vector $\vec{t}$ is sufficient for trapping any starting point.

Algorithm 1 *Rotation Index Algorithm*

Require: *a starting point $\mathcal{P}_0$ of the curve c, which is not a singular point; a tracing step size L; an empty stack;*
  $n_c \Leftarrow 1$; {Initialize the rotation index.}
  $\vec{t} \Leftarrow$ tangent vector of the curve at $\mathcal{P}_0$;
  $i \Leftarrow 1$;
  repeat
    $p \Leftarrow \mathcal{P}_{i-1} + L\,\vec{t}$;
    $\mathcal{P}_i \Leftarrow$ improved coordinates of p through Newton iterations;
    if *$\mathcal{S}_1$ and $\mathcal{S}_2$ are tangential at $\mathcal{P}_i$* ***then***
      Determine the singular point P;
      if *P is not in the stack* ***then***
        push P in the stack;
        allocate to P a cell for storing the multiplicity ($g \Leftarrow 1$) and the algebraic sum of the exterior angles ($sum \Leftarrow 0$);
      else
        $g \Leftarrow g + 1$;{Increment the multiplicity of P.}
        if *P is a branch point* ***then***
          pop out all the branch generators in the stack till the closest matcheable branch generator;
          in- or decrement n_c according to the orientation of the loop; {Update the rotation index with regard to the parametrized loops.}
          $n_c \Leftarrow n_c$ - $\frac{sum}{2\pi}$;{Restore the rotation index.}
          Update the algebraic signed sum (sum) of the exterior angles of the parametrized loops adjacent to $c^{-1}(P)$;
          $n_c \Leftarrow n_c$ + $\frac{sum}{2\pi}$;{Update the rotation index with regard to the new sum of the exterior angles.}
        end if
      end if
    else
      $\vec{t} \Leftarrow$ tangent vector at $\mathcal{P}_i$
    end if
    Increment i
  until *the local geometric properties of $\mathcal{P}_0$ and $\mathcal{P}_i$ are almost the same.*
  $\mathcal{P}_n \Leftarrow \mathcal{P}_i$ {Store the terminating point.}

Exahustive tests have shown that, if the starting point is not a singular point, the closeness and the tangent matching conditions are sufficient local geometrical prop-

erties for evaluating the terminating point $\mathcal{P}_n$ with respect to the starting point $\mathcal{P}_0$, namely,

Closeness condition: $\| \mathcal{P}_0\mathcal{P}_n \| < \epsilon$.

Tangent matching condition: $|\frac{\overrightarrow{t_{\mathcal{P}_0}}}{\|\overrightarrow{t_{\mathcal{P}_0}}\|} \cdot \frac{\overrightarrow{\mathcal{P}_n\mathcal{P}_0}}{\|\overrightarrow{\mathcal{P}_n\mathcal{P}_0}\|} - 1| < \epsilon$, where $\overrightarrow{t_{\mathcal{P}_0}}$ is the tangent vector of the curve at $\mathcal{P}_0$.

In this section we present a modified marching algorithm which integrates the proposed rotation index algorithm in the marching algorithm with circular steps proposed by Wu and Andrade [18]

Algorithm 2 *Marching Algorithm with Circular Steps*

Require: *a starting point $\mathcal{P}_0$; its adjacent point on the intersection curve $\mathcal{P}_1$; the arc angle L*
$\overrightarrow{t_0} \Leftarrow$ tangent vector at $\mathcal{P}_0$;
$\overrightarrow{t_1} \Leftarrow$ tangent vector at $\mathcal{P}_1$;
$i \Leftarrow 2$
repeat
Determine, on the basis of $\mathcal{P}_{i-2}$, $\mathcal{P}_{i-1}$, $\overrightarrow{t_{i-2}}$, and $\overrightarrow{t_{i-1}}$, a point p on the aproximating osculating circle of $\mathcal{P}_{i-1}$ with the angle $\widehat{p\mathcal{P}_{i-1}}$ equal to L;
$\mathcal{P}_i \Leftarrow$ improved coordinates of p with Newton iterations;
$\overrightarrow{t_i} \Leftarrow$ tangent vector at $\mathcal{P}_i$;
Increment i;
until *$\overrightarrow{t_i}$ is not defined.*

Wu and Aléssio sketched in [16] the estimation of the rotation index from the singular points that are met while marching along a curve c defined implicitly by two regular surfaces $\mathcal{S}_1$ and $\mathcal{S}_2$. We may use the parametric domain of either $\mathcal{S}_1$ or $\mathcal{S}_2$ for computing the rotation index, when the curve is closed in both of the domains. Although this index is subjected to modifications while the curve is traced, one can use the intermediate values to distinguish the potential terminating points and to adaptatively adjust the step size, in such a way that the starting point $\mathcal{P}_0$ cannot be overcrossed. The potential terminating points are the points for which the algebraic sum $\sum$ of the variations of the tangent vectors in the chosen parametric domain satisfies the rotation index condition:

Rotation Index condition: $|\sum -2n_c\pi| < \eta$.

This slight modification has not only avoided over-tracing but has also improved the performance of the tracing procedure as well: We may trace with large step size whenever we are not in the vicinity of a potential terminating point and the local geometrical conditions should only be evaluated when we are in the vinicity of a potential terminating point.

Algorithm 3 *Modified Marching Algorithm*

Require: *a starting (regular) point $\mathcal{P}_0$; its adjacent (regular) point on the intersection curve $\mathcal{P}_1$; ϵ (closeness and tangent matching conditions); η (rotation index condition); arc angle L; an empty stack;*

$n_c \Leftarrow 1$; {*Initialize the rotation index.*}

$\sum \Leftarrow 0$; {*Initialize the sum of the variations of tangent vectors.*}

$\Delta \Leftarrow L$; {*Initialize the arc angle.*}

$\overrightarrow{t_0} \Leftarrow$ *tangent vector at* $\mathcal{P}_0$;

$\overrightarrow{t_1} \Leftarrow$ *tangent vector at* $\mathcal{P}_1$;

$i \Leftarrow 2$

repeat

Determine, on the basis of $\mathcal{P}_{i-2}$, $\mathcal{P}_{i-1}$, $\overrightarrow{t_{i-2}}$, *and* $\overrightarrow{t_{i-1}}$, *a point p on the aproximating osculating circle of* $\mathcal{P}_{i-1}$ *with the angle* $\widehat{p\mathcal{P}_{i-1}}$ *equal to* Δ;

$\mathcal{P}_i \Leftarrow$ *improved coordinates of* p *through Newton iterations;*

if $\mathcal{S}_1$ *and* $\mathcal{S}_2$ *are tangential at* $\mathcal{P}_i$ ***then***

Determine the singular point P;

if P *is not in the stack* ***then***

push P *in the stack;*

allocate to P *a cell for storing the multiplicity (*$g \Leftarrow 1$*) and the algebraic sum of the exterior angles (*$sum \Leftarrow 0$*);*

else

$g \Leftarrow g + 1$; {*Increment the multiplicity of* P.}

if P *is a branch point* ***then***

pop out all the branch generators in the stack till the matcheable branch generator;

in- or decrement n_c *according to the orientation of the loop;* {*Update the rotation index with regard to the parametrized loops.*}

$n_c \Leftarrow n_c$ - $\frac{sum}{2\pi}$; {*Restore the rotation index.*}

Update the algebraic signed sum (sum*) of the exterior angles of the parametrized loops adjacent to* $c^{-1}(P)$ *in the parametric domain of* $\mathcal{S}_1$;

$n_c \Leftarrow n_c$ + $\frac{sum}{2\pi}$; {*Update the rotation index with regard to the new sum of the exterior angles.*}

end if

end if

end if

$\overrightarrow{t_i} \Leftarrow$ *tangent vector at* $\mathcal{P}_i$;

Increment $\sum$ *by the amount of variation of* $\overrightarrow{t_{i-1}}$ *to* $\overrightarrow{t_i}$ *in the parametric domain of* $\mathcal{S}_1$;

if $|\sum -2n_c\pi| < \eta$ *&* $\parallel \mathcal{P}_0\mathcal{P}_i \parallel < 100\epsilon$ *& branch generators are paired &* $\Delta = L$ ***then***

$\Delta \Leftarrow \frac{\epsilon}{2}$;

else if $|\sum -2n_c\pi| > \eta$ *&* $\Delta = \frac{\epsilon}{2}$ ***then***

$\Delta \Leftarrow L$;

end if

Increment i

until *($|\sum -2n_c\pi| < \eta$ & each brach point in the stack has at least two branch generators & $\| \mathcal{P}_0\mathcal{P}_{i-1} \| < \epsilon$ & $|\frac{\overrightarrow{t_{\mathcal{P}_0}}}{\|\overrightarrow{t_{\mathcal{P}_{i-1}}}\|} \cdot \frac{\overrightarrow{\mathcal{P}_{i-1}\mathcal{P}_0}}{\|\overrightarrow{\mathcal{P}_{i-1}\mathcal{P}_0}\|} - 1| < \epsilon$) $\vee$ ($\overrightarrow{t_{i-1}}$ is not defined).*

5 Examples

To illustrate how the proposed modified marching algorithm works, we present in this section some numerical results. We set $\epsilon = 0.001$, η = 0.5 and initialize the arc angle with $L = 0.1 radians$. For each example we present three figures: the intersection curve in R^3 and their pre-images in the parametric domains of the regular surfaces from which the curve is defined implicitly.

The first pair of surfaces to be tested is the following: (Figure 13)

$S_{11}(u, v)$: $F(u, v) = (u, v, 0.2 * u^4 + 0.1 * v^4)$
$S_{12}(s, w)$: $G(s, w) = (s, w, 0.3 * s^2 * w - 0.1 * w^2 + 0.2 * w^3)$.

These surfaces define implicitly a curve which is regularly homotopic to a C_2 curve.

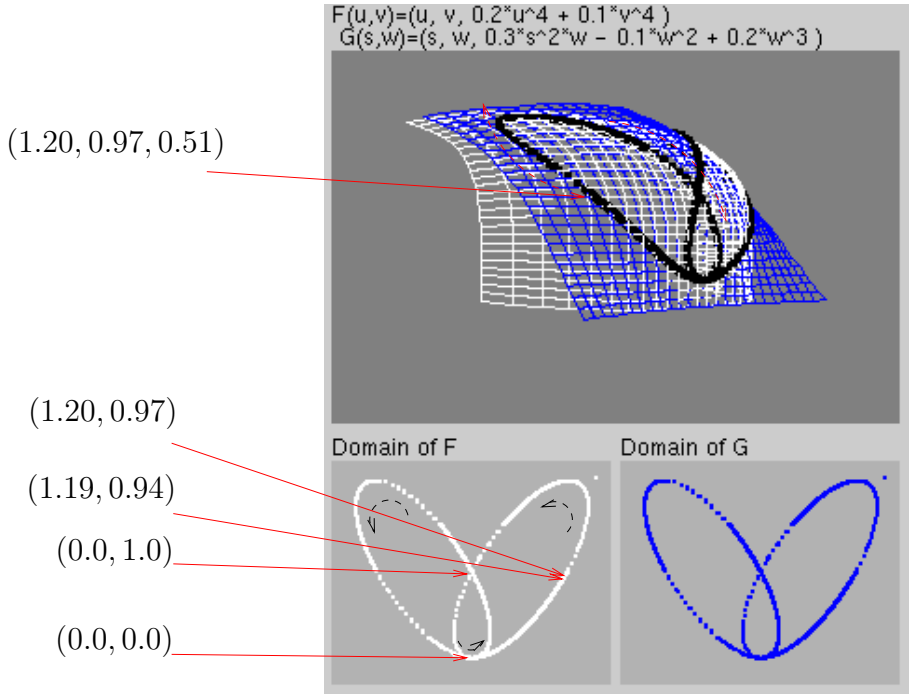

Figure 13. Intersection of S_{11} and S_{12}.

Tracing starts at the point $S_{11}(1.20, 0.97)$=$(1.20, 0.97, 0.51)$. When the branch point $S_{11}(0.0, 1.0)$ is passed, it is pushed into the stack. Progressing the marching, the tangential point $(0.0, 0.0)$ is reached before we return to the branch point $S_{11}(0.0, 1.0)$ and complete a turn along a (positively oriented) parametrized loop. Hence, n_c is incremented by 1. Further steppings with $L = 0.1$ are performed till the point $(1.19, 0.94)$, when the sum of variations of the tangent vectors in the parametric domain of S_{11} becomes 12.554 ($|12.554 - 2n_c\pi| = 0.01 < 0.5$), its distance to the point $(1.20, 0.97)$ is $0.03 < 0.1$ and there is a pair of branch generators associated to the point $S_{11}(0.0, 1.0)$. Therefore, the arc angle is reduced for approaching carefully the starting point $(1.20, 0.97)$ in the parametric domain of S_{11}. The terminating point we reached is 0.0003 far from the starting point and its tangent vector makes an angle of 0.00006 with respect to the tangent vector at the starting point.

The second pair of surfaces to be considered is the following: (Figure 14)

$S_{21}(u, v)$: $F(u, v) = (u, v, (u^2 + v^2)^2 + 3 * u^2 * v - v^3)$
$S_{22}(s, w)$: $G(s, w) = (s, w, 0)$.

Their intersection results in curves with a triple point in R^3 and in the parametric domains. All of them are regularly homotopic to a C_2 curve.

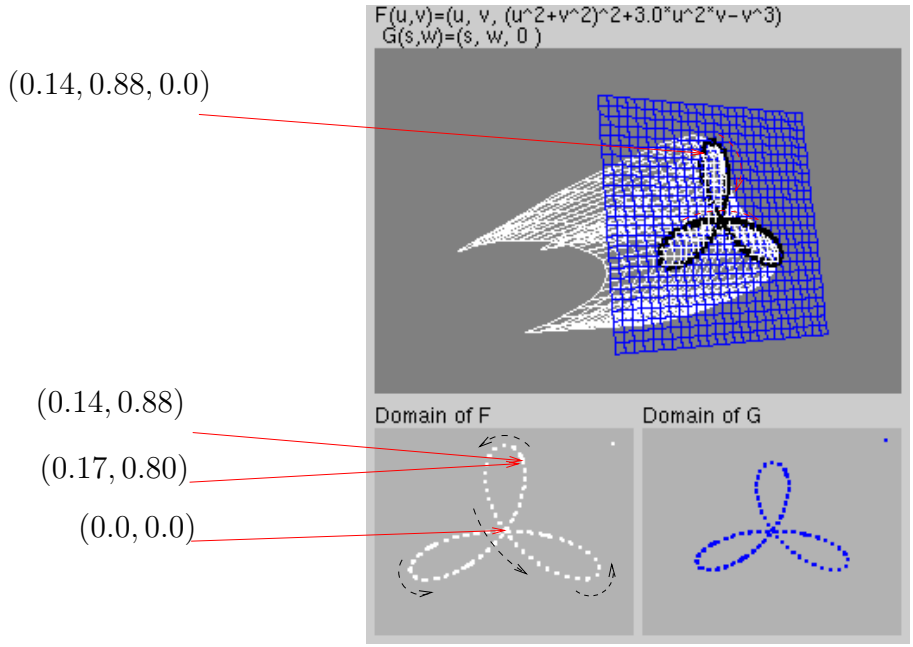

Figure 14. Intersection of S_{21} and S_{22}.

Tracing starts at the point $S_{21}(0.14, 0.88)$=$(0.14, 0.88, 0.0)$. The branch point $S_{21}(0.0, 0.0)$ is passed three times while the curve is traced: (1) $S_{21}(0, 0, 0.0)$ is pushed into the stack; (2) the second branch generator is added and the sum of the exterior angles, in the parametric domain of S_{21}, of the two potential parametrized loops adjacent to this point is updated (sum = 1.8925 - 1.8925 = 0); (3) the third branch generator

is included, the algebraic sum of the exterior angles at this point is updated again (sum = $1.8925 + 1.8925 + 2.4980 \approx 6.283 \approx 2\pi$), and the rotation index is accordingly adjusted (n_c = 3 (parametrized loops) - $\frac{2\pi}{2\pi}$ = 2). At the point $(0.17, 0.80)$, the sum of the tangent vector variations in the parametric domain satisfies the rotation index condition ($|12.3923 - 2n_c\pi| = 0.17 < 0.5$), its distance to $(0.14, 0.88)$ is 0.0784, and all the branch generators of $S_{21}(0, 0, 0.0)$ are paired. Hence, the arc angle L is narrowed. The iteration stops at a parametric point whose distance to the starting point is 0.0004 and whose tangent vector makes the angle of 0.0005 in relation to the tangent vector at the starting point. We remark that we used the discriminant method proposed by Ye and Maekawa [19] to get precisely three tangent directions at the branch point $S_{21}(0.0, 0.0)$.

The third pair of surfaces to be considered is as follows: (Figure 15)

$S_{31}(u, v)$: $F(u, v) = (u, v, (3u^2 + 3v^2))$
$S_{32}(s, w)$: $G(s, w) = (s, 5(s^2 + w^2) - 1, w + 1)$.

Their intersection determines in the parametric domains a pair of disjoint simple curves.

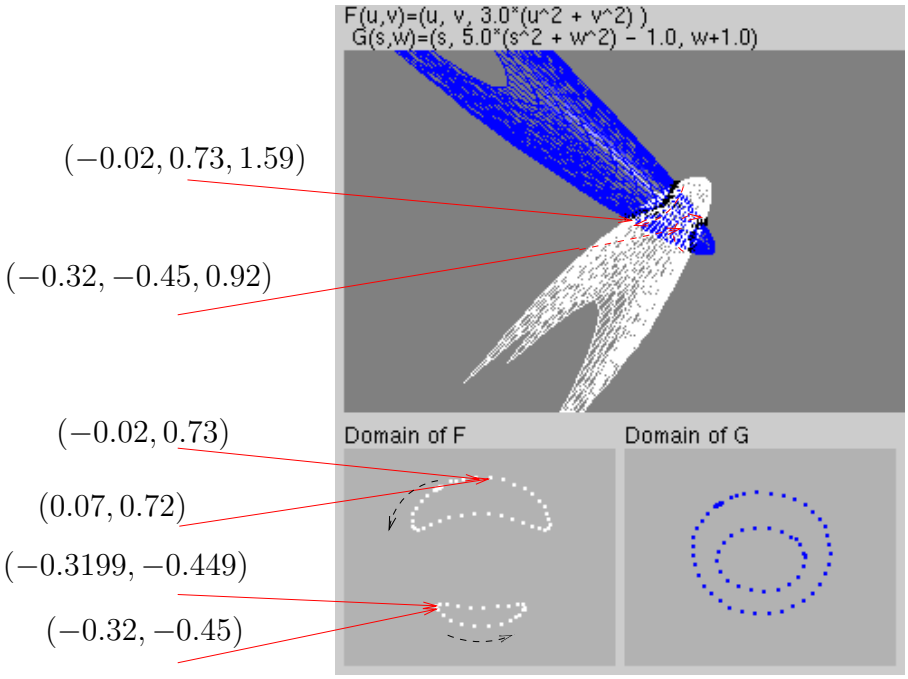

Figure 15. Intersection of S_{31} and S_{32}.

The subdivision scheme was used to obtain the two starting points. From the point $S_{31}(-0.32, -0.45)$=$(-0.32, -0.45, 0.92)$, the smaller closed curve was traced, while the bigger one was traced from the point $S_{31}(-0.02, 0.73)$=$(-0.02, 0.73, 1.59)$. Along the smaller curve, the program identifies that the sum of the tangent vector variations in the parametric domain of S_{31} reaches 5.818606 at a point very

close to $(0.32, -0.45)$, which satisfies the rotation index condition (in this case, n_c = 1). The distance of this point to the starting domain point is 0.009238. The arc angle is reduced until the terminating point. Analogously, the step size is shortened at the point $(0.07, 0.72)$ for the bigger simple curve (when the sum of the tangent vectors and the distance are, respectively, 6.13 and 0.092).

The final intersection to be analyzed is the following: (Figure 16)

$S_{41}(u, v)$: $F(u, v) = (u, v, v^4 - v^2 + 2 * u^2)$
$S_{42}(s, w)$: $G(s, w) = (s, w, s^4)$.

The intersection is a Devil's curve consisting of two open and one closed curves in the parametric domain.

The subdivision scheme was applied to obtain the three starting points on each of these curves: $S_{41}(1.38, 0.50)$, $S_{41}(-0.34, 0.83)$ and $S_{41}(-1.37, 0.82)$. From the point $S_{41}(-0.34, 0.83)$=$(-0.34, 0.83, 0.01)$ the central eight-shaped curve is traced. When the branch point $S_{41}(0.0, 0.0)$ is passed at the second time, the rotation index n_c is decremented by 1 as the newly built parametrized loop is negatively oriented with respect to the loop that contains the starting point. At the point $(-0.31, 0.87)$ the variations of the tangent vectors sum up -0.0197, satisfying the rotation index condition and its distance to the point $(-0.34, 0.83)$ is 0.048. Hence, the arc angle is reduced till the terminating point, whose distance to the starting point is almost 0.

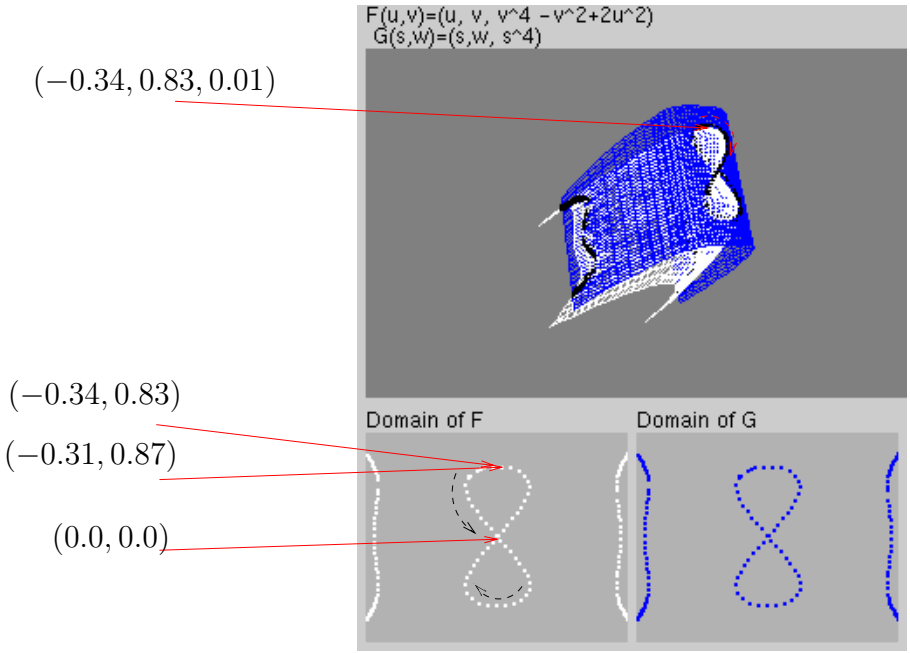

Figure 16. Intersection of S_{41} and S_{42}.

6 Concluding Remarks

We presented an expression for computing a rotation index of a piecewise regular closed plane curve on the basis of its parametrized loops and its branch points with net multiplicity greater than 2 (Eq. 1). A formal proof that validates this result is given. An algorithm that implements the expression is developed and integrated to a marching-based surface–surface intersection procedure for tracing with circular steps a closed loop without overlapping. Differently from the local differential properties commonly used in SSI algorithms, the rotation index is a global geometrical property which reflects the behavior of the traced curve. This allows us to trace it efficiently and reliably.

We point out that the problems may arise in our proposed modified marching algorithm, if the intersection surfaces generate two or more curves that intersect each other, as shows Figure 17. The curve c_1 self-crosses at $\mathcal{P}_1$ and crosses the curve c_2 at $\mathcal{P}_2$, $\mathcal{P}_3$, $\mathcal{P}_4$ and $\mathcal{P}_5$. If the tracing is started from $\mathcal{P}_0$, the branch points $\mathcal{P}_4$ and $\mathcal{P}_5$ will remain in the stack when we go back to $\mathcal{P}_0$ after completing one turn.

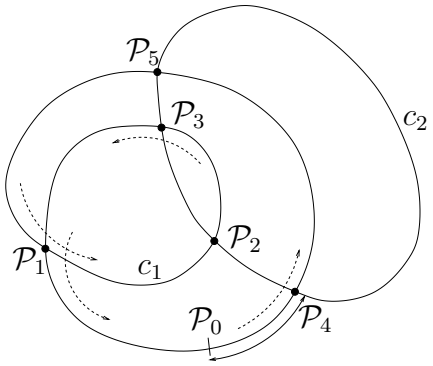

Figure 17. Intersections between two curves.

Figure 18.a illustrates the two intersecting simple curves, both in R^3 and in the parametric domain, that are defined implicitly by the regular surfaces

$S_{51}(u,v)$: $F(u,v) = (u, v, u^4 - u^2 + v^4 - v^2)$
$S_{52}(s,w)$: $G(s,w) = (s, w, -0.25)$.

In the current version of our program, four turns are performed before it stops appropriately.

To remedy such problems, we propose to overcross the arc $\mathcal{P}_0\mathcal{P}_4$ in Figure 17 for ensuring that the parametrized loop $\mathcal{P}_4\mathcal{P}_5\mathcal{P}_1\mathcal{P}_0\mathcal{P}_4$ closes on the branch point $\mathcal{P}_4$, that is, the last branch generator matches the first branch generator of $c_1^{-1}(\mathcal{P}_4)$ regarding the tracing sense. This extension will be considered in the next version of our program.

In general, an algorithm for distinguishing self-intersection points of a regular curve is not trivial. It involves computation of equations of higher order. Nevertheless, if a curve is defined as the intersection of two regular surfaces, those points can be detected by imposing the necessary condition of collinearity of their normal vectors and, if the curve contains singularities up to fourth contact order without abrupt change of normal directions, the marching algorithm proposed by Wu and Andrade [18] deliver reliable results even in the neighborhood of a singular point.

When the singularity of the curve has contact order greater than 4, the marching scheme with circular steps may fail, as exemplifies Figure 18.b. In this case, the osculating circles of the two branches that cross at the oscnode $(0.0, 0.0)$ have almost the same radii. Therefore, when the approximant to the curve in the vicinity of $(0.0, 0.0)$ is refined with Newton iterations, it converges to the wrong branch and the wrong result is delivered: two tangential simple curves requiring two starting points. We believe that we may overcome this problem by classifying the nature of singular points [6] and the marching algorithm may be benefited from the incorporation of this classification, as already remarked by Bajaj et al. [2]. Some preliminary tests with singular points of type A_k, $k \leq 5$, support our idea. As further work, we will go deeper into the singularity theory to exploit its potential in predicting the number and the directions of the bifurcations at each singular point. Finally, we point out that this may open the possibility to trace curves containing cusps after slight modifications in Eq. 1.

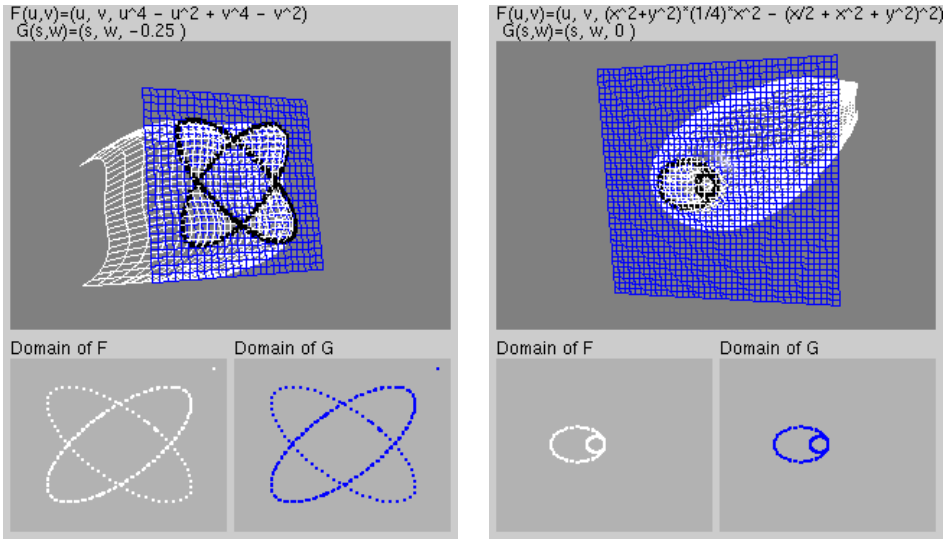

(a) (b)

Figure 18. Open Problems: (a) Intersection with other curves, and (b) Contact order greater than 4.

Acknowledgements

We would like to thank the anonymous referres for the critical and constructive comments and for the helpful suggestions that greatly improve the first version of this paper. We would also to acknowledge a doctoral fellowship provided by the National Council for Scientific and Technological Development (CNPq) in the period 1998–2001 to the author Osmar Aléssio for this research project (Grant N^o 145149/1998-6). The third author Sueli I. Costa aknowledges the State of São Paulo Research Foundation (FAPESP/Grant N^o 02/07473-7) and the National Council for Scientific and Technological Development (CNPq/Grant N^o 304573/2002-7) for supporting her research.

References

[1] C. Asteasu. Intersection of arbitrary surfaces. *Computer-Aided Design*, 20:533–538, 1988.

[2] C. L. Bajaj, C. M. Hoffmann, J. E. Hopcroft, and R.E. Lynch. Tracing surface intersections. *Computer Aided Geometric Design*, 5(4):285–307, 1988.

[3] R. E. Barnhill, G. Farin, M. Jordan, and B.R.Piper. Surface/surface intersection. *Computer Aided Geometric Design*, 4(1–2):3–16, 1987.

[4] R. E. Barnhill and S. N. Kersey. A marching method for parametric surface/surface intersection. *Computer Aided Geometric Design*, 7(1–4):257–280, 1990.

[5] M. Berger and B. Gostiaux. *Differential Geometry: Manifolds, Curves, and Surfaces*, volume 1. Springer-Verlag, 1988.

[6] J. W. Bruce and P. JU. Giblin. *Curves and Singularities*. Cambridge-University Press, 2nd edition, 1992.

[7] M. P. Carmo. *Differential geometry of curves and surfaces*. Prentice Hall Inc., New Jersey, 1st. edition, 1976.

[8] W. Klingenberg. *A Course in Differential Geometry*. Springer-Verlag, 2nd edition, 1978.

[9] S. Krishnan and D. Manocha. An efficient surface intersection algorithm based on lower-dimensional formulation. *ACM Transactions on Graphics*, 16(1):74–106, 1997.

[10] G. Müllenheim. On determining start points for a surface/surface intersection algorithm. *Computer Aided Geometric Desgin*, 8(5):401–408, 1991.

[11] T. W. Sederberg, H. N. Christiansen, and S. Katz. An improved test for closed loops in surfaces intersections. *Computer Aided Design*, 21(8):505–508, 1989.

[12] T. W. Sederberg and R. J. Meyers. Loop detection in surface patch intersections. *Computer Aided Geometric Design*, 5(2):161–171, 1988.

[13] P. Sinha, E. Klassen, and K. K. Wang. Exploiting topological and geometric properties for selective subdivision. In *Proc. ACM Symp. Computational Geometry*, pages 39–45, 1985.

[14] Tz. E. Stoyanov. Marching along surface/surface intersection curves with an adaptative step length. *Computer Aided Geometric Desgin*, 9(6):485–489, 1992.

[15] D. J. Struik. *Lectures on Classical Differential Geometry*. Dover Publications, Inc., 2nd. edition, 1961.

[16] S.-T. Wu and O. Aléssio. Complete and non-overlapping marching along a closed regular intersection curve. *Computers & Graphics*, 26(6):853–864, 2002.

[17] S. T. Wu, O. Aléssio, and S. I. R. Costa. On estimating local geometric properties of intersection curves. In *Proceedings of SIBGRAPI 2000*, pages 152–159, 2000.

[18] S. T. Wu and L. N. de Andrade. Marching along a regular surface/surface intersection with circular steps. *Computer Aided Geometric Design*, 16(4):249–268, 1999.

[19] X. Ye and T. Maekawa. Differential geometry of intersection curves of two surfaces. *Computer Aided Geometric Design*, 16(8):767–788, 1999.